MOLECULAR AND CELLULAR BIOLOGY, Oct. 2002, p. 7313–7324 Vol. 22, No. 20
0270-7306/02/$04.00+0 DOI: 10.1128/MCB.22.20.7313–7324.2002

Mouse Af9 Is a Controller of Embryo Patterning, Like Mll, Whose Human Homologue Fuses with AF9 after Chromosomal Translocation in Leukemia

Emma C. Collins, Alexandre Appert, Linda Ariza-McNaughton,† Richard Pannell, Yoshihiro Yamada,‡ and Terence H. Rabbitts*

MRC Laboratory of Molecular Biology, Cambridge CB2 2QH, United Kingdom

Received 14 May 2002/Returned for modification 11 July 2002/Accepted 17 July 2002

Chromosomal translocation t(9;11)(p22;q23) in acute myeloid leukemia fuses the *MLL* and *AF9* genes. We have inactivated the murine homologue of *AF9* to elucidate its normal role. No effect on hematopoiesis was observed in mice with a null mutation of *Af9*. However, an *Af9* null mutation caused perinatal lethality, and homozygous mice exhibited anomalies of the axial skeleton. Both the cervical and thoracic regions were affected by anterior homeotic transformation. Strikingly, mice lacking functional *Af9* exhibited a grossly deformed atlas and an extra cervical vertebra. To determine the molecular mediators of this phenotype, analysis of *Hox* gene expression by in situ hybridization showed that *Af9* null embryos have posterior changes in *Hoxd4* gene expression. We conclude that the *Af9* gene is required for normal embryogenesis in mice by controlling pattern formation, apparently via control of *Hox* gene regulation. This is analogous to the role of *Mll,* the murine homolog of human *MLL*, to which the *Af9* gene fuses in acute myeloid leukemias.

The consequence of chromosomal translocations in human cancer is to cause enforced expression of proto-oncogenes or the creation of tumor-specific fusion genes (reviewed in reference 52). Chromosomal translocations often involve transcription regulators (9) which function as master regulators of cell fate in their normal situations of expression (53). Human AF9 was identified as one of the most common fusion partners of the mixed-lineage leukemia protein (MLL, also called HTRX and ALL-1) (14, 20, 63, 70) and is most usually associated with acute myeloid leukemias (AML). MLL fusion proteins are present in approximately 10% of acute lymphoid leukemias and myeloid leukemias (42) and in up to 80% of leukemias in infants (33, 51), as well as in 85% of cases of secondary leukemias developing after treatment of a primary tumor with alkylating agents or topoisomerase II inhibitors (3, 8, 61). In an individual leukemia, the fusion protein results from one of a variety of reciprocal chromosomal translocations, causing the association of upstream exons of the *MLL* gene on chromosome 11, band q23, with downstream exons of the partner gene, generally on a separate chromosome. *MLL* is a human homologue of *Drosophila melanogaster trithorax* (*trx*), a master homeotic gene regulator essential for normal patterning during embryo development (2, 43). Gene-targeting studies have demonstrated a similar role for *MLL* in mammals (17, 21, 67, 69).

More than 30 different *MLL* fusions have been identified (28), and these code for a structurally and functionally heterogeneous group of proteins (reviewed in references 1 and 10). However, different MLL fusion proteins are consistently associated with hematopoietic tumors of different lineages. Thus, whereas *MLL-AF9* is mainly found in AML, the translocation involving the *AF4* gene (16, 20, 47) occurs almost exclusively in tumors of the B-cell lineage. This suggests that the fusion partner plays a role in determining disease phenotype, either because it influences the site and timing of the translocation itself or because the mutation has a cell-autonomous effect on a specific subpopulation. The active role of the fusion partner has been further confirmed by experiments demonstrating that mice carrying a knock-in allele of *Mll-AF9*, in which human *AF9* sequences were fused to one allele of mouse *Mll*, have been shown to develop AML similar to those occurring in human patients (12, 15). Moreover, the product of the analogous t(11;19) translocation, MLL-ENL (48, 55, 63, 68), when used in retroviral transduction (39), transforms murine bone marrow cells, and both the transcriptional transactivation activity of ENL and the DNA-binding motifs of MLL are required for the oncogenic properties of the fusion protein (59). Recently, the putative role in determining tumor phenotype was reinforced by the generation of an *Af4* null mutant mouse, which revealed that the *Af4* gene, associated with lymphoid malignancy following chromosomal translocation in humans, plays a role in early lymphoid development (30).

The function of the AF9 protein is unknown. It contains a serine- and proline-rich domain, as well as a nuclear localization signal, consistent with a role as a transcription factor (29). AF9 also contains a sequence possessing transcriptional activation properties, which is consistently retained by MLL-AF9 fusion proteins. Moreover, AF9 has regions of extensive homology to both ENL and yeast ANC1 (65). Interestingly, ANC1 has been shown to be involved in the yeast RNA polymerase II transcription complex, as well as the SWI/SNF chromatin-remodeling complex, a multisubunit complex believed to facilitate transcription activator access by disrupting nucleo-

* Corresponding author. Mailing address: MRC Laboratory of Molecular Biology, Hills Rd., Cambridge CB2 2QH, United Kingdom. Phone: 01223-402286. Fax: 01223-412178. E-mail: thr@mrc-lmb.cam.ac.uk.

† Present address: CRUK, Lincolns Inn Fields, London WC2A 3PX, United Kingdom.

‡ Present address: Department of Pathology and Biology of Diseases, Kyoto University Graduate School of Medicine, Kyoto 606-8501, Japan.

somes in an ATP-dependent manner (7, 13, 50). The homology of AF9 and ENL to ANC1 has led to the proposal that these proteins may interact with a human SWI/SNF complex, and the fusion proteins may retain these features (5, 6).

We have investigated the function of the *Af9* gene by homologous recombination in the mouse. The *Af9* null mutation was found to have an effect on the formation of the axial skeleton, suggesting that *Af9* plays a role in embryo-patterning processes. While heterozygous *Af9* mutant mice were normal and fertile and exhibited no segment anomalies, homozygous gene disruption led to anterior transformation of the cervical and thoracic regions and to early postnatal lethality. The presence of an eighth cervical vertebra generally compensated for the lack of a thoracic vertebra. Thus Af9 is required for normal segmentation in embryo development.

MATERIALS AND METHODS

Gene targeting and generation of chimeric mice. For the construction of targeting vector pAf9LZ, a 6.5-kb *Bgl*II fragment containing the first two coding exons of mouse *Af9* (designated exons 1 and 2; see Fig. 1) was isolated from a 129/Sv/E library in λ phage 2001. This fragment was subcloned into the linker *Hin*dIII site of pMC1-TK (62) by blunt-end ligation. A 5-kb *Bam*HI fragment from vector pBS-TAG_3/IRESlacZ/lox/MC1neoPA/lox (gift from Karen Douglas and Andrew Smith) was subsequently inserted into a *Hin*dIII site in *Af9* exon 2 by blunt-end ligation. This cassette contained the encephalomyocarditis virus internal ribosome entry site (IRES), followed by the *lacZ* and *neo* sequences, the latter flanked by *loxP* sites. Embryonic stem (ES) cells were transfected as described previously (64). CCB ES cells were grown on neomycin-resistant mouse embryonic feeders during selection. Af9LZ ES cells were transfected with expression vector pPGKCrebpA (gift from Andrew McKenzie) for the removal of the *neo* cassette by transient expression of Cre recombinase to generate Af9NO clones and grown on mouse embryonic feeders without selection.

DNA from ES cells and from mouse tissues was prepared with Puregene (Gentra Systems). Ten micrograms of DNA was digested with a restriction enzyme and resolved on 0.8% agarose gels. After electrophoresis, the DNA was transferred to nylon membranes and hybridized to radioactive probes as described previously (41). Homologous recombinant Af9LZ clones were identified by using a nonrepetitive, 2-kb *Eco*RI-*Bgl*II genomic fragment as an external probe (5′ probe). Positive clones were confirmed by using an external 3′ probe consisting of a 1-kb *Bgl*II-*Bam*HI fragment and by hybridization with an internal *neo* probe to exclude multiple insertions. Af9NO genomic DNA was analyzed with the 3′ probe and the internal *neo* fragment.

Clones Af9LZ and Af9NO were injected into C57BL/6 blastocysts. High-percentage male chimeras were mated with wild-type C57BL/6 females, and the resulting offspring were assayed for germ line transmission of the *Af9LZ* and *Af9NO* alleles by filter hybridization of tail DNA with the 5′ and 3′ probes, respectively.

RNA extraction and RT-PCR analysis. Extraction of total RNA from whole mouse embryos was carried out with Trizol (Gibco-BRL). cDNA was generated with SuperRT reverse transcriptase (RT; HT Biotechnology). cDNA from 5 μg of total RNA was diluted to 100 μl. One microliter of cDNA in a reaction volume of 25 μl was subjected to 35 cycles of PCR amplification with *Af9* primers 5′-GGCTAGCTCGTGTTCCG-3′ and 5′-GGTGGATCTTTGCACAC-3′. Temperature cycling was 95°C for 1 min, 65°C for 1 min, and 72°C for 1 min.

Immunophenotyping of hematopoietic cells in *Af9* null mice. Single-cell suspensions were prepared from bone marrow, spleens, and thymuses of Af9LZ mice and wild-type controls and stained with fluorescent antibodies followed by fluorescence-activated cell sorter analysis. The following antibodies were used: B220, Gr-1 (spleen cells), CD4, CD8 (thymus cells), CD44, Ter119, Gr-1, Mac-1, and c-Kit (bone marrow cells).

β-Galactosidase staining of whole embryos. β-Galactosidase staining of mouse embryos was carried out according to published protocols (23). Pregnant females were sacrificed by lethal injection, and embryos were dissected from the uterine horns. Embryonic day 10.5 (E10.5) and E11.5 embryos were prefixed in 4% paraformaldehyde (PFA) in phosphate-buffered saline (PBS) for 30 min at room temperature. E12.5 and E14.5 embryos were prefixed in 4% PFA in PBS supplemented with 0.25% Nonidet P-40 for 45 min and 1 h, respectively. Embryos were subsequently washed three times with PBS for 10 min each before addition of 2 ml of freshly prepared X-Gal (5-bromo-4-chloro-3-indolyl-β-D-galactopyranoside) staining solution (0.2% X-Gal, 2 mM $MgCl_2$, 5 mM $K_3Fe[CN]_6$). After incubation at 37°C for 24 h, X-Gal was removed by repeated rinsing in PBS, and embryos were postfixed in 4% PFA at room temperature for 48 h. Embryos were rinsed in PBS and equilibrated in 30% sucrose in PBS supplemented with 0.05% azide for long-term storage at 4°C.

Skeletal preparations of newborn mice. Skeletons of newborn mice were stained for cartilage with Alcian blue and for bone with Alizarin red as described previously (23). Newborn mice were sacrificed by lethal injection. Specimens were skinned, eviscerated, and fixed in 95% ethanol for 3 to 5 days and then incubated at room temperature for 24 h in Alcian blue stain (15 mg of Alcian blue in 80 ml of 95% ethanol–20 ml of glacial acetic acid). Samples were rinsed twice in 95% ethanol for 24 h each. Specimens were cleared by being placed in 1% KOH for approximately 6 h and counterstained overnight with Alizarin red stain (50 mg of Alizarin red per liter of 2% KOH). Finally, samples were cleared by being placed in 2% KOH solutions of decreasing strengths. Initially, specimens were placed in 2% KOH for 2 to 3 days, and the clearing process was completed in solutions having the following ratios of 2% KOH to glycerol for 24 h each: 80:20, 40:60, and 20:80. Samples were stored indefinitely in 2% KOH–glycerol (20:80).

Whole-mount RNA in situ hybridization. Mouse embryos were obtained by crossing heterozygous Af9NO mice and genotyped by filter hybridization of yolk sac DNA. They were fixed overnight in 4% PFA–PBS and whole-mount in situ hybridization was carried out as described previously (66). *Hox* gene riboprobes were made by using cDNA fragments previously described and labeled with digoxigenin (46). *Cdx-1* has been described (60), and the *Cdx-4* probe was derived from a 520-bp cDNA fragment encoding the 5′ part of the translated sequence and finishing just before the homeobox domain. This fragment was obtained by RT-PCR on mouse E8.5 embryo total RNA with primers having the following sequences (26): 5′-ATGTACGGAAGCTGTCTTTTGGAG-3′ and 5′-CTTTTGTCCTGGTTTTCCCCGTCAC-3′.

RESULTS

Generation of *Af9* null mutant mice. The physiological role of endogenous Af9 was investigated in mice with a null mutation of *Af9*. A targeting vector (pAF9LZ) was constructed in which the second coding exon of mouse *Af9* was disrupted by inserting an IRES–β-galactosidase gene (IRES-*lacZ*) cassette as an expression marker and a neomycin resistance cassette (*neo*) as a positive selection marker (Fig. 1A). ES cells were transfected with pAF9LZ, and two independent, homologous recombinant clones were identified by filter hybridization (Fig. 1B). One of these was used to generate chimeric mice and in turn germ line heterozygous carriers of the null *Af9* mutation (designated Af9LZ mice). Furthermore, to eliminate any possible interference of the *neo* gene enhancer with *lacZ* expression patterns, the Cre-*loxP* system of phage P1 (22) was used to remove the *neo* sequence (flanked in the targeting cassette by *loxP* sites) from the second of these targeted Af9LZ ES clones to generate the Af9NO clone (Fig. 1A). High-percentage chimeric mice were generated from this clone, and the transmission of the disrupted alleles to their offspring was verified by filter hybridization.

Heterozygous *Af9* mutant mice from the two independent *Af9*-targeted ES clones (i.e., Af9LZ and Af9NO) appeared normal and fertile and were bred to generate homozygous mice. Twenty-five percent of mice observed at birth were of the $Af9^{-/-}$ genotype, showing that the null mutants survive embryogenesis. The absence of functional Af9 in these animals was verified by RT-PCR, confirming the lack of the *Af9* transcript in $Af9^{-/-}$ mutants (Fig. 1C). However, no homozygous mutant animals survived to weaning age. Approximately 50% of $Af9^{-/-}$ mice identified were found dead at birth or within hours thereafter. The remaining homozygous mutants generally became severely runted and died in the first 2 weeks. No

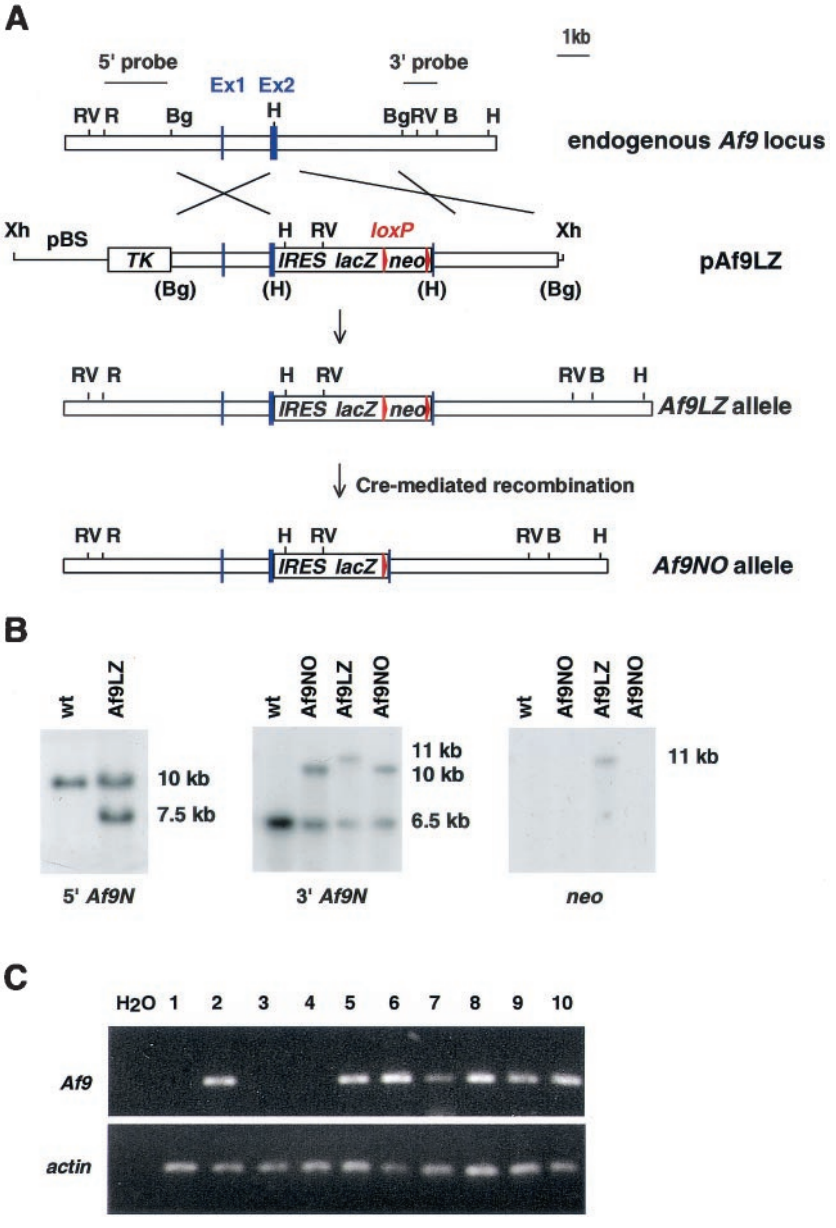

FIG. 1. Targeting strategy for the generation of *Af9* null alleles. (A) A partial genomic map of the mouse *Af9* gene around the two exons encoding the first 64 amino acids of mouse *Af9* (designated exons 1 and 2) is shown in the top line. Targeting vector pAf9LZ (second line) contained a 6.5-kb genomic *Bgl*II fragment, with a 5-kb *lacZ-neo* cassette inserted into a *Hin*dIII site in exon 2. The IRES sequence allowed independent translation of the *Escherichia coli lacZ* gene, which served as an *Af9* gene expression marker. The *neo* sequence conferred G-418 resistance, allowing positive selection of targeted ES cells. This sequence was flanked by *loxP* sites to allow subsequent excision by transient expression of Cre recombinase (the starting vector was a gift from K. Douglas and A. Smith). Upstream of the targeting fragment, the herpes simplex virus thymidine kinase gene (*TK*) cassette allowed negative selection of nonhomologous integration events (62). The regions of homology with the endogenous *Af9* gene are indicated. The mutant *Af9* allele (*Af9LZ*) resulting from homologous recombination is illustrated in the third line. The *Af9NO* allele, resulting from transient expression of Cre recombinase, is illustrated in the fourth line. H, *Hin*dIII; B, *Bam*HI; Bg, *Bgl*II; R, *Eco*RI; RV, *Eco*RV; Xh, *Xho*I. Blue boxes, exons; red arrowheads, *LoxP* sites. (B) Filter hybridization analysis of ES clones. A 2-kb nonrepetitive *Eco*RI-*Bgl*II fragment 5′ of the targeted region (A) detected a 10-kb *Eco*RV fragment in the wild-type (wt) genomic DNA, reduced to 7.5 kb in the *Af9LZ* allele (left). A nonrepetitive 3′ probe consisting of a 1-kb *Bgl*II-*Bam*HI fragment (A) detected a 6.5-kb wild-type *Hin*dIII band, increased to 11 kb in *Af9LZ* and then reduced to 10 kb in *Af9NO* (center). The same 11-kb *Af9LZ* band hybridized with a probe specific for the inserted *neo* cassette (right); a single *neo* insertion was observed. This band was not visible in the *Af9NO* clones after removal of the *neo* sequence by expression of Cre recombinase. (C) RT-PCR analysis of RNA from a representative litter of E11.5 Af9NO embryos was used to detect the presence of the *Af9* transcript. PCRs were analyzed on agarose gels. PCR carried out with no DNA template (H_2O) served as a negative control. A 207-bp band amplified from the *Af9* mRNA was generated from all samples, except those from embryos 1, 3, and 4, which were null *Af9* mutants. Actin gene-specific RT-PCR, indicating that all cDNA populations analyzed were of comparable quality and concentration, is shown below. Embryo numbers are indicated above the gel. Embryos 1, 3, and 4 were $Af9NO^{-/-}$, while the remaining embryos were either $Af9NO^{+/-}$ (2, 5, and 7 to 9) or wild type (6 and 10).

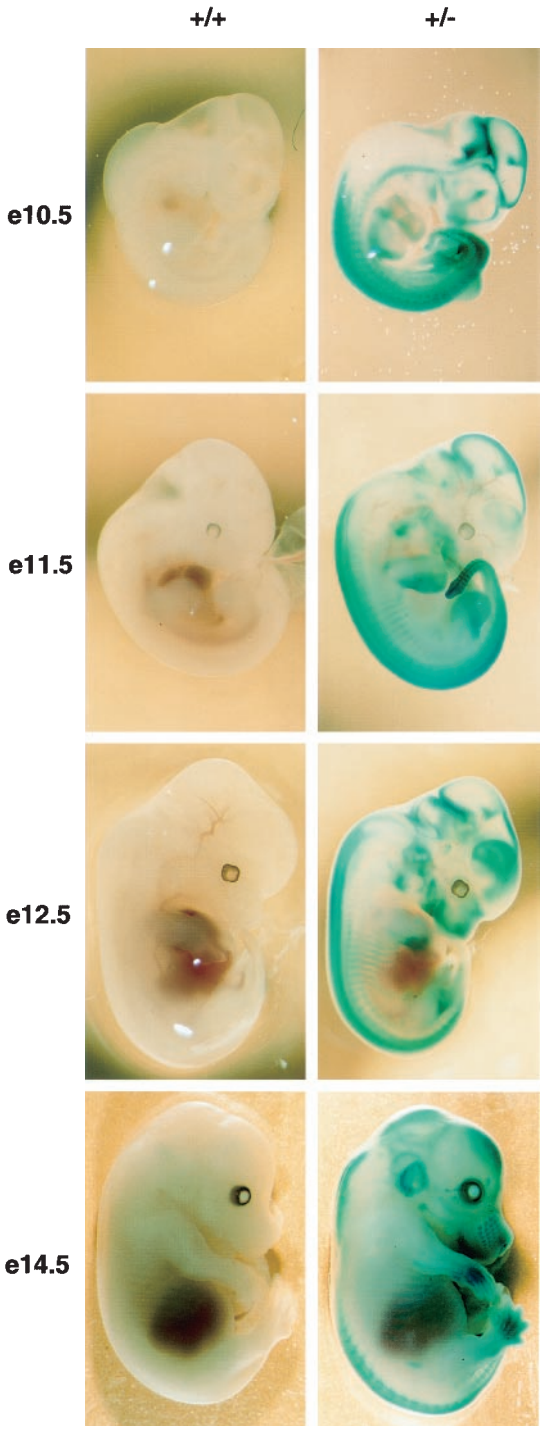

FIG. 2. Af9 expression in embryogenesis detected by β-galactosidase staining of Af9LZ mouse embryos. Af9LZ heterozygous mice were mated with C57BL/6 mice, and staged embryos were removed from the uterus, prefixed in 4% PFA, and stained with X-Gal solution overnight. Wild-type embryos (+/+) and heterozygous littermates (+/−) were examined at E10.5, E11.5, E12.5, and E14.5. Activity of the *Af9* gene, leading to expression of the β-galactosidase gene in the *Af9LZ* allele, is visible as blue staining. No staining by endogenous β-galactosidase was observed in the wild-type controls. Areas of precartilage primordium, such as the developing jaw, nose, and skull, as well as the limb buds, developing ribs, and vertebrae, exhibited *Af9* expression, particularly at the later stages of development. At E14.5, the external ear and the vibrissae also exhibited strong *Af9* expression.

obvious external malformations or internal changes to organs were observed. Moreover, hematopoiesis appeared normal in newborn $Af9^{-/-}$ animals, as analyzed by histology and flow cytometry (data not shown). *AF9* mRNA transcripts are mainly detected in cell lines of megakaryocytic and erythroid origins, which does not correlate with the myeloid specificity of MLL-AF9-induced tumors (29). Together with the apparently unaffected hematopoiesis of the $Af9^{-/-}$ mice, this suggests that the primary function of Af9 is not to regulate genes that are normally active in myeloid cells.

Af9 is highly expressed in the developing skeleton during embryogenesis. Our mutant *Af9LZ* allele contained an IRES-*lacZ* reporter, allowing assessment of *Af9* expression patterns during embryogenesis. Figure 2 shows β-galactosidase staining of heterozygous Af9LZ embryos taken at E10.5, E11.5, E12.5, and E14.5, with wild-type littermates as negative controls. X-Gal staining was observed in the developing skeletal system of limb buds, prevertebrae, rib anlagen, developing jaw, nose, and skull. Staining was also observed in the vibrissae, gut, and forming genital organs, as well as parts of the developing neural system, in particular in the caudal hindbrain and at the midbrain-hindbrain border. Identical staining patterns were obtained with the Af9LZ and Af9NO strains, the latter lacking the *neo* gene, indicating that the *neo* enhancer had no effect on *lacZ* or *Af9* expression (Fig. 3A) and confirming the concordance of expression in the two independent lines. Hence, the β-galactosidase activity observed reflects normal *Af9* gene expression.

β-Galactosidase staining patterns of homozygous *Af9* mutants were also investigated and compared with those of heterozygous littermates (Fig. 3B). A subtle difference could be observed in the cervical region at E14.5, a stage of development in which cartilage and bone formation has begun. In $Af9^{-/-}$ embryos, expression along the developing axial skeleton appeared to extend to a more anterior limit than in $Af9^{+/-}$ specimens, as well as appearing slightly broader. Otherwise staining patterns appeared similar in $Af9^{-/-}$ and $Af9^{+/-}$ specimens, and no obvious malformations were observed.

Af9 homozygous mutants exhibit homeotic transformations of the axial skeleton. Since β-galactosidase staining results indicated significant *Af9* expression in developing bony structures, skeletons of *Af9* mutants were analyzed for possible anomalies. Long bone structures of $Af9^{-/-}$ animals appeared normal, as assessed by histology analysis (data not shown). However, whole-skeleton preparations of newborn animals, stained for cartilage and bone with Alcian blue and Alizarin red, revealed abnormalities of the axial skeletons of homozygous mutants (Fig. 4). While heterozygous Af9LZ and Af9NO specimens appeared normal, the homozygous knockout mice were generally lacking a pair of floating ribs and the associated vertebra, having a total number of 12 instead of 13 pairs of ribs and vertebrae (Fig. 4). Only 1 out of 13 skeletons from $Af9^{-/-}$ pups had a 13th thoracic vertebra, but this carried very small rib anlagen. Moreover, the ribs of $Af9^{-/-}$ pups were not at-

Strong staining was also observed in neural tissues, especially the caudal hindbrain, the midbrain-hindbrain junction, and the sympathetic ganglia, as well as in the heart tube, at E10.5.

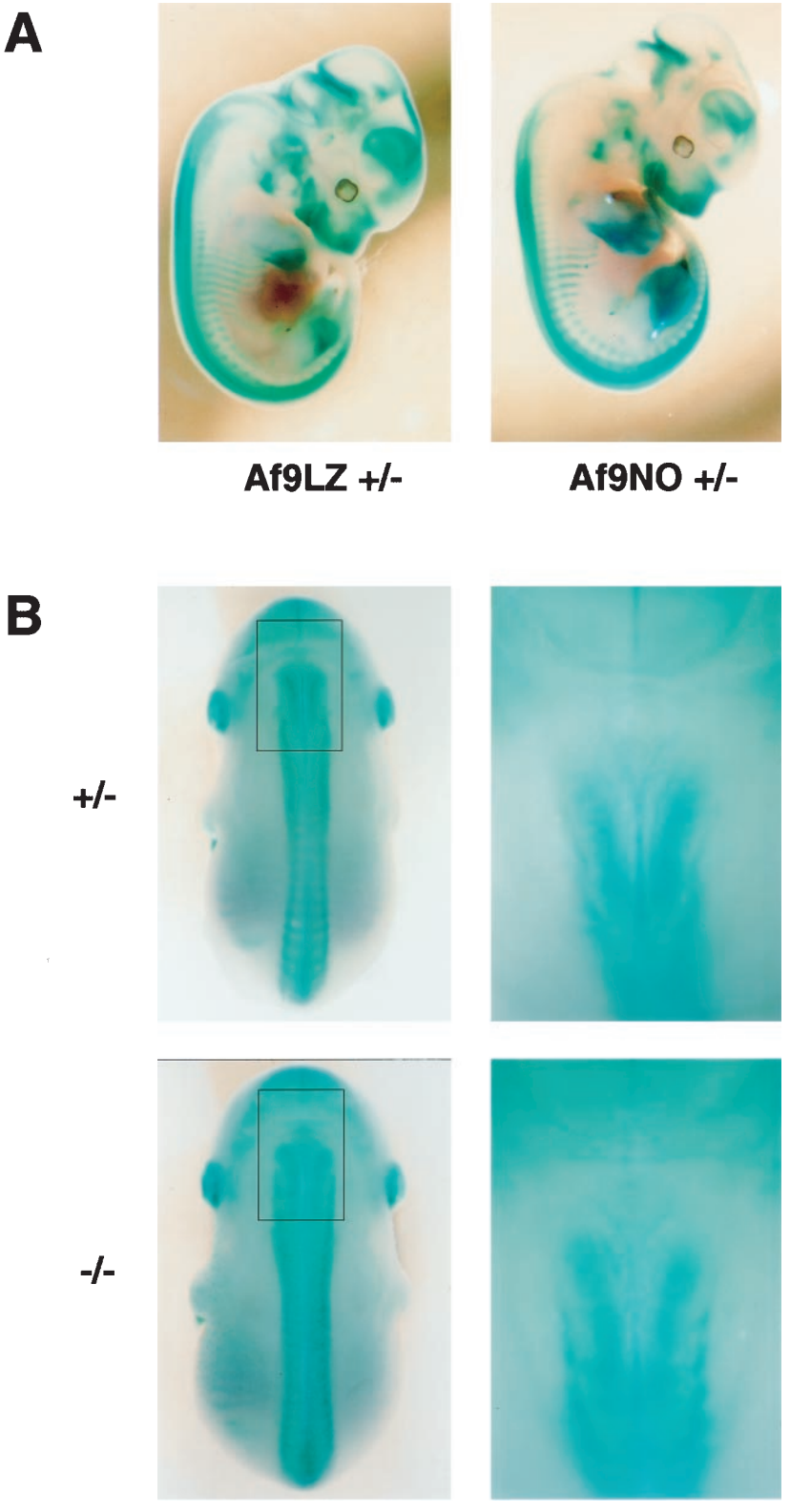

FIG. 3. Effect of homozygous *Af9* mutation on embryonic development. Heterozygous Af9LZ or Af9NO mice were mated, and embryos were removed at E12.5 (A) or E14.5 (B). All embryos were prefixed in 4% PFA and stained with X-Gal solution overnight. (A) Comparison of β-galactosidase staining patterns of Af9LZ and Af9NO heterozygous embryos at E12.5. Similar staining patterns were observed with both lines. (B) Comparison of β-galactosidase staining patterns of heterozygous and homozygous Af9NO embryos. An $Af9NO^{+/-}$ embryo (top) is compared with an $Af9NO^{-/-}$ embryo (bottom; E14.5). A dorsal view of each embryo is shown on the left, with an enlargement of the cervical region on the right. Staining along the axial skeleton extended to a more anterior limit in the homozygous *Af9* mutants. In addition, the structures exhibiting *Af9* expression appeared to spread over a broader lateral area in this region.

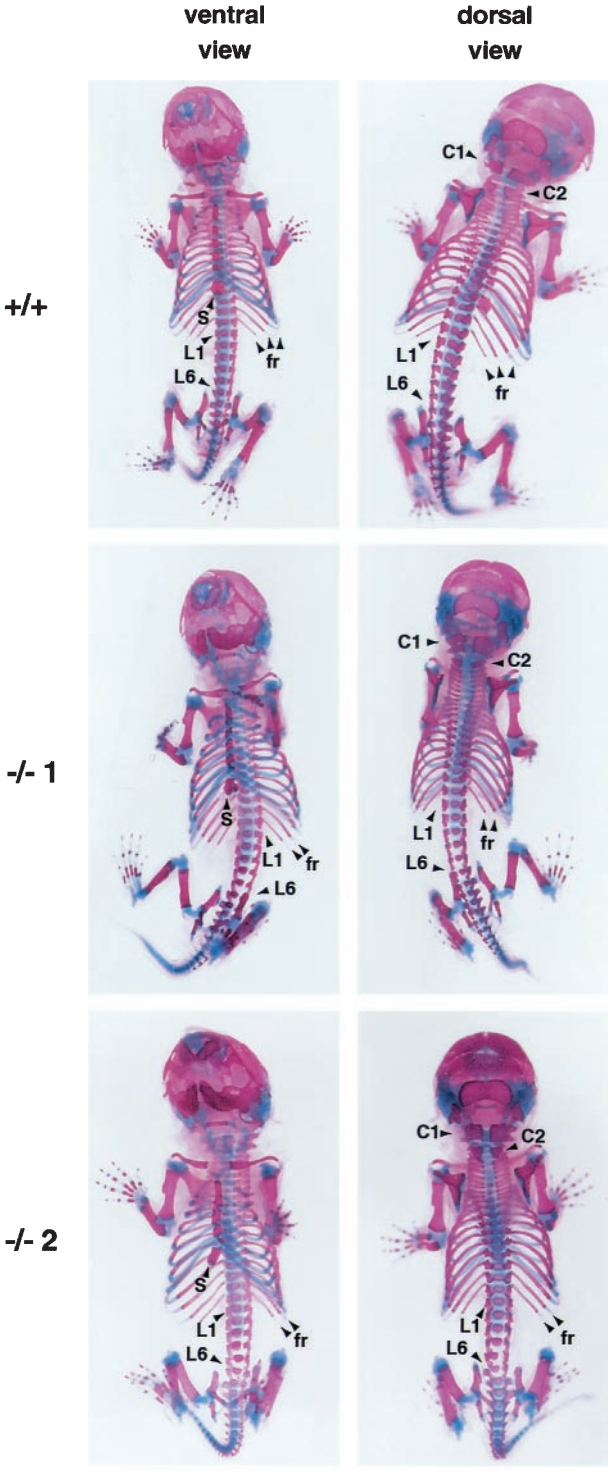

FIG. 4. Skeletal development in *Af9* mutant mice. Skeletons of newborn Af9LZ pups were cleared in 2% KOH and stained for bone with Alizarin red and for cartilage with Alcian blue. A wild-type control mouse (+/+) is shown together with two homozygous *Af9* mutant specimens (−/− 1 and 2). Ventral and dorsal views are shown. Among the anomalies observed in the homozygous mutant mice was a lack of the third pair of floating ribs (fr) and malformations of the first and second cervical vertebrae (C1 and C2). Moreover, articulated ribs did not join the sternum (s) pairwise but rather in a staggered, disorganized fashion, resulting in sternum malformations of various levels of severity (see in particular specimen −/− 2). C1, atlas; C2, axis; L1 and L6, first and last lumbar vertebrae, respectively.

tached to the sternum in pairs but rather were staggered randomly (Fig. 4). Consequently, sternums were deformed, consisting mainly of bone rather than of segments of bone separated by cartilage, as observed in normal newborn mice.

When the forelimbs and shoulder blades were removed, we observed that 11 out of 13 skeletons from $Af9^{-/-}$ mice also presented eight cervical vertebrae, compensating for the missing thoracic vertebra, instead of the normal seven, common to almost all mammals (Fig. 5B and D). In the remaining two $Af9^{-/-}$ samples, the second vertebra or axis had the appearance of two vertebrae partially fused dorsally (Fig. 5C). One of these was the same specimen that presented a 13th pair of ribs, raising the possibility that this represented a milder penetrance of the phenotype. Furthermore, vertebra C2 was malformed to various degrees even in the specimens where it was not fused to the third vertebra (Fig. 5).

In addition to the presence, complete or partial, of the extra cervical vertebra, the first vertebra or atlas also had the appearance of two partially fused vertebrae (Fig. 5). In all 13 $Af9^{-/-}$ specimens analyzed, the atlas was approximately twice as high as in wild-type pups, with lateral gaps. The vertebral body extended the whole height of the vertebra, making it substantially larger than those in the wild-type controls. Hence, *Af9* knockout mice appeared to possess eight cervical vertebrae, as well as an additional, partially duplicated structure. This unprecedented situation makes the numbering and nomenclature of vertebrae in the $Af9^{-/-}$ pups somewhat subjective. For descriptive purposes, the misshapen double atlas was labeled C1, the following structure, resembling a normal axis in most $Af9^{-/-}$ specimens, was designated C2, and the following cervical vertebrae were designated C3 to C8. Thus, in two of the $Af9^{-/-}$ skeletons, vertebrae C2 and C3 were considered partially fused.

In most wild-type mice, vertebra C6 carried a pair of cervical ribs, joined to the first pair of thoracic ribs, themselves joined to the sternum (Fig. 5). This was not observed in homozygous *Af9* knockout mice; however, vertebra C8 usually carried a pair of rib anlagen (Fig. 5), which were not attached to the sternum or to the ribs on the first thoracic vertebra. Moreover, the spinous process normally present on thoracic vertebra T2 was usually observed on T3 (Fig. 5). Finally, in the C3-to-C8 region, the cervical spine was noticeably compressed, causing an S-shaped deformation of the neck and a forward tilt of the head in comparison with the $Af9^{+/+}$ samples. This may contribute to the early postnatal death of the homozygous mutant pups, due to respiratory and/or feeding difficulties as well as possible neurological problems.

Individually dissected, stained vertebrae of an Af9LZ$^{-/-}$ newborn pup and a wild-type control littermate are shown in Fig. 6 (all cervical vertebrae as well as T1 are shown). The atlas and the axis (C1 and C2) of $Af9^{-/-}$ animals had cross-section shapes similar to those of the controls. However, in normal mouse vertebrae C3, C4, and C5 have practically identical morphologies. In the $Af9^{-/-}$ specimen, the third vertebra was more similar to C2 than to C4, with a round rather than an oval shape, and instead C4, C5, and C6 appeared almost indistinguishable. Thus, an anterior shift in identity was observed from the third vertebra onwards. The appearance of cervical vertebrae C7 and C8 in the $Af9^{-/-}$ pups was consistent with this observation as, like those of C6 and C7 in the wild-type pups,

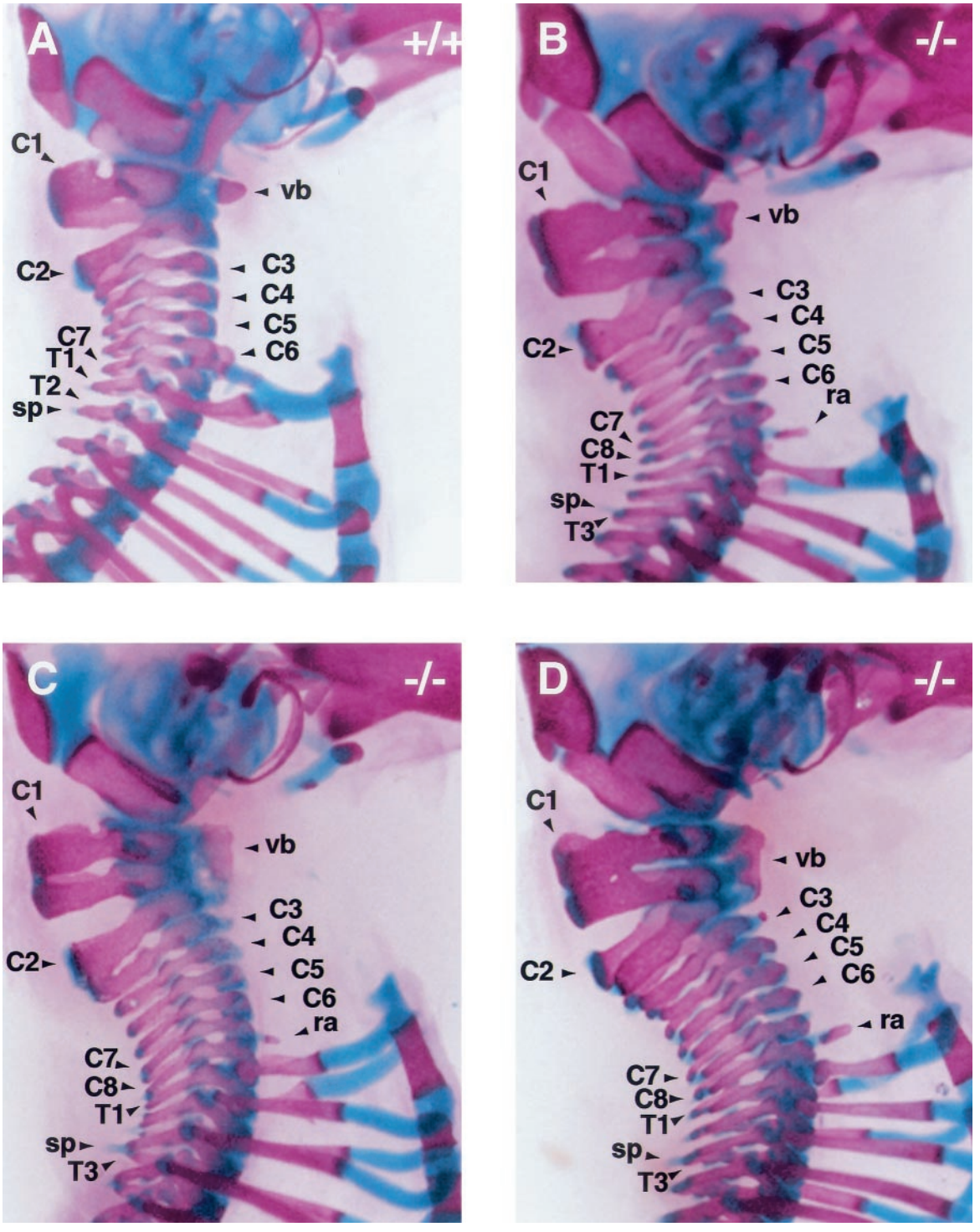

FIG. 5. Cervical skeletons of *Af9* mutant mice. The cervical regions of skeletons of newborn Af9LZ mice, stained with Alizarin red and Alcian blue, were examined after removal of the forelimbs and shoulder blades. (A) Wild-type (+/+) control mouse; (B to D) homozygous *Af9* mutant specimens. The atlases (C1) of *Af9* knockout mice were severely deformed; each had the appearance of two vertebrae partially fused, with a single vertebral body (vb) extending along both substructures. Moreover, most *Af9* mutants exhibited a complete, supplementary cervical vertebra, bringing the total number of cervical vertebrae to eight, as opposed to the normal seven (B and D). Occasionally, the third vertebra (C3) was partially fused to C2, but with a vertebral body of its own (C). In addition, *Af9* knockout mice generally exhibited small protruding rib anlagen (ra) on vertebra C8, whereas wild-type controls usually had a pair of cervical ribs on C6. Furthermore, the spinous process (sp) normally found on the second thoracic vertebra was observed on T3 instead. C1 to C8, cervical vertebrae; T1 to T3, first thoracic vertebrae.

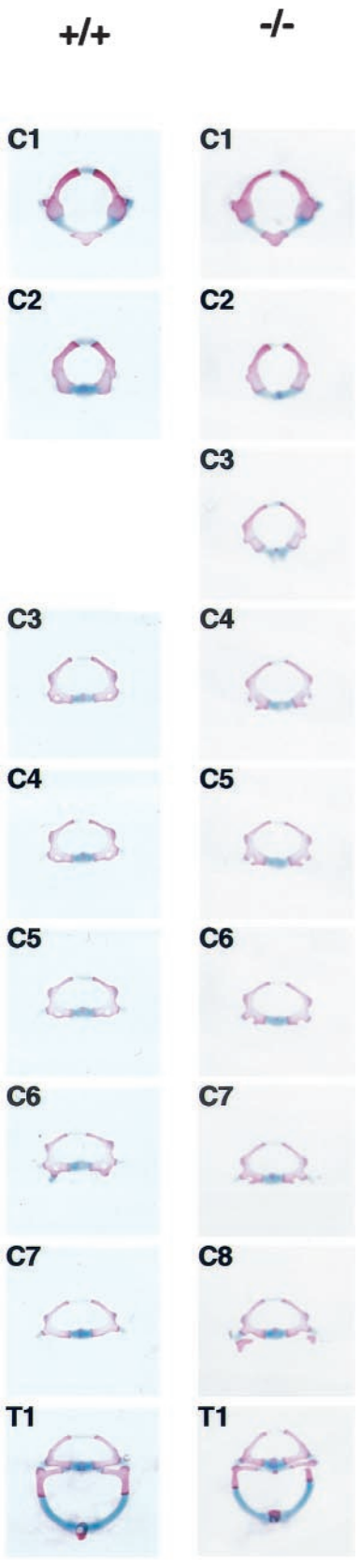

FIG. 6. Morphology of individual vertebrae of *Af9* mutant mice. Vertebrae from the cervical and thoracic regions of stained skeletons of newborn Af9LZ mice were dissected and examined under a microscope. Samples from a homozygous *Af9* knockout animal (−/−) and the corresponding segments from a wild-type control mouse (+/+) are shown. All cervical vertebrae (C1 to C8) and the first thoracic vertebra (T1) are shown. The third vertebra of *Af9* mutants exhibited C2 characteristics, while C4 to C8 resembled C3 to C7 in the wild type.

the shapes of C7 and C8 in the $Af9^{-/-}$ mutants progressed toward that of a thoracic vertebra, with C8 even carrying small rib anlagen.

Thus, it appeared that an anterior homeotic transformation of the axial skeleton had occurred throughout most of the cervical region and the entire thoracic region, resulting in the shift of C3→C2 through to T13→T12, with the third cervical vertebra possibly resulting from a duplication of the C2 segment. In addition, the gross deformation of C1 seemed to indicate the presence of another extra vertebral segment fused to the atlas. In contrast, the number and morphology of all the lumbar and caudal vertebrae as well as the appendicular skeleton, were apparently normal.

Af9 null mutation affects *Hoxd-4* gene expression. The homeotic transformation observed in *Af9* null mice suggests a role for *Af9* as a master gene controlling expression of downstream effector genes such as *Hox* and *Cdx* genes. Such a role has been shown for Mll (69), the common fusion partner of Af9 in leukemia-associated chromosomal translocations. Accordingly expression patterns of specific *Hox* genes in wild-type, heterozygous, and $Af9^{-/-}$ embryos were compared by whole-mount in situ hybridization. We examined *Hoxa2*, *-a3*, *-a4*, *-b2*, and *-b3* as well as *Cdx1* and *Cdx4*. A caudal shift in the anterior expression boundary of *Hoxd4* was detected in E9.5 $Af9^{-/-}$ embryos compared with wild-type or heterozygous specimens (Fig. 7). At this stage, *Hoxd4* expression normally reaches an anterior limit localized between rhombomeric segments r6 and r7 (19, 27), but in $Af9^{-/-}$ embryos the anterior limit of *Hoxd4* expression was localized between r7 and r8 (Fig. 7). In both wild-type and heterozygous embryos (the latter not shown), the *Hoxd4* staining extended to the normal expression boundary localized between rhombomeric segments r6 and r7. In the $Af9^{-/-}$ embryos, a posterior shift of the anterior expression limit was observed, corresponding to approximately one rhombomeric segment. We did not find evidence for alterations of the other *Hox* genes analyzed or for alterations of *Cdx1* or *Cdx4* expression.

DISCUSSION

Af9 may be an upstream master regulator of genes involved in embryo patterning. The skeletal abnormalities exhibited by *Af9* null mutant mice suggest a role in embryo patterning. The transformations of homeotic character observed in individual vertebrae are reminiscent of, but distinct from, phenotypes obtained with aberrant expression of genes such as members of the vertebrate *HOX* family of homeobox genes (for a review see reference 38). Experimental alteration of *Hox* gene expression in transgenic or knockout mice (44) or by maternal exposure to retinoic acid (34, 36) results in homeotic transformations of the axial skeleton. For instance, several *Hox* gene null mutants exhibit an effect that mirrors the *Af9* null mutation,

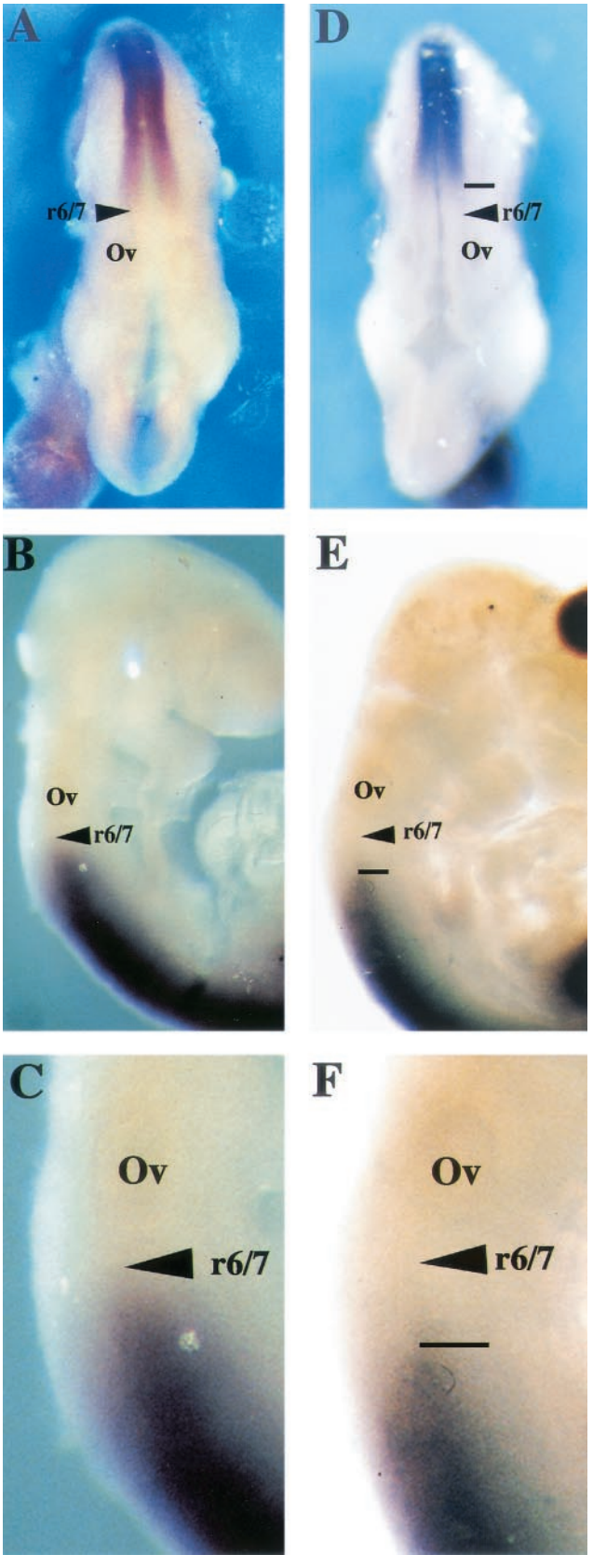

FIG. 7. *Hoxd4* gene expression in *Af9* null mutant embryos. *Hoxd4* expression was analyzed by whole-mount in situ hybridization (66) of wild type (A to C) and $Af9^{-/-}$ (D to F) E9.5 embryos. A *Hoxd4* riboprobe was made from a cDNA fragment and labeled with digoxigenin (46). (A and D) Dorsal views; (B, C, E, and F) lateral views. (C and F) Magnification (×2.5) of the specimens from panels B and E. In wild-type embryos, the *Hoxd4* staining extended to a boundary localized between rhombomeres r6 and r7. In the $Af9^{-/-}$ embryos, a posterior shift of the anterior expression limit, corresponding to approximately one rhombomere, was observed. Ov, otic vesicle.

namely, the posterior transformation of C7 into T1, complete with a pair of ribs. This effect is observed in *Hoxa4*, *Hoxa5*, and *Hoxa6* mutants and at low frequency in $Hoxd4^{-/-}$ mutants (24, 25, 31, 37), suggesting that the C7-T1 junction may be particularly susceptible to perturbations in *Hox* gene expression. The first two vertebrae, the atlas and the axis, are also frequent targets of homeotic transformation following *Hox* gene deregulation. Loss of either *Hoxb4* or *Hoxd4* function leads to a partial posterior homeotic transformation of C1 to C2 (25, 54), whereas disruption of *Hoxd3* causes anterior transformations of these two vertebrae (11). Interestingly, overexpression of *Hoxa7* also results in the atlas and the axis acquiring the characteristics of more-posterior vertebrae, as well as, in the presence of an additional vertebra, the proatlas (35). In wild-type mice, the proatlas anlage is a temporary embryonic structure which subsequently contributes cells to the basioccipital bone, but, following *Hoxa7* overexpression, this structure appears to undergo a partial transformation to a vertebral fate.

Unlike the phenotypes observed with aberrant expression of individual *Hox* genes, the homeotic transformations exhibited by *Af9* null mutant mice were spread along the embryo axis from the first cervical vertebra to the last thoracic segment. This suggests that *Af9* may play a role as a master regulator, perhaps of *Hox* genes. Indeed, in many respects the characteristics of $Af9^{-/-}$ mice were found to be remarkably similar to those of mice carrying null mutations of *Hox* gene regulator *Cdx1* (60). *Cdx1* expression is established at E7.5 and subsequently regresses in a temporally controlled fashion along the entire embryo (45, 60). Homozygous disruption of *Cdx1* leads to axial skeletal abnormalities with anterior homeotic transformation, and in situ hybridization analysis of various *Hox* genes has demonstrated a posterior shift of their expression domains by one segment in the *Cdx1* null mutants (60).

The similarities between the *Af9* and *Cdx1* mutant phenotypes suggest that they may have a regulatory effect on related groups of target genes, presumably *Hox* genes. Nonetheless, important differences were observed, and in particular the *Af9* phenotype appeared more severe than that of *Cdx1*. First, disruption of *Af9* was lethal shortly after birth, whereas $Cdx1^{-/-}$ mice are viable and fertile. Moreover, the homeotic transformation in the *Af9* knockout mice extended throughout the thoracic region, with the last pair of ribs missing, whereas no morphological changes are apparent posterior to T9 in $Cdx1^{-/-}$ animals. In addition, while *Cdx1* mutants exhibit an incomplete first vertebra, partly fused to the basioccipital bone, the atlases of *Af9* mutants showed a grossly deformed, duplicated structure. This was presumably due either to a fusion of the atlas with a persisting proatlas or to a duplication of the developing C1 structure in embryogenesis.

In view of the homeotic transformation phenotype of *Af9* null mutant mice it seems likely that Af9 plays a role in the

regulation of genes involved in the complex processes of embryo patterning. Comparison with the effects observed following aberrant expression of *Hox* genes suggests that Af9 may affect the activity of these genes, directly or indirectly. In particular, striking parallels between the *Af9* phenotype and the effects of null mutations of *Hox* gene members of the paralogous group 4 (notably *Hoxa4*, *Hoxb4*, and *Hoxd4*) suggested a possible effect on the expression of these genes (24, 25, 37, 54). Indeed, the in situ hybridization experiments illustrated in Fig. 7 demonstrated a posterior shift in the anterior expression limits of *Hoxd4* in E9.5 $Af9^{-/-}$ embryos. This effect is similar to that observed with expression in *Cdx1* null mutant embryos (60) and confirms that Af9 affects *Hox* gene expression, directly or indirectly.

A link between *Af9* and *Mll* genes, embryo patterning, and leukemia. AF9 is a common partner of MLL in AML. Interestingly, the skeletal phenotype of the *Af9* knockout mouse is reminiscent of that observed in mice with a disruption of the *Mll* gene (69), indicating that both genes play a crucial role in embryo-patterning processes. Homozygous *Mll* inactivation is lethal by E11; however, $Mll^{+/-}$ mice are viable, though they exhibit growth retardation and hypofertility. Heterozygous *Mll* mutants are haploinsufficient and display segment abnormalities, with disordered identity observed in the cervical, thoracic, and lumbar regions. Anterior transformations are present in the cervical and upper thoracic regions, while posterior transformations are observed in the lower thoracic, lumbar, and sacral regions. All specimens lack either a thoracic or a lumbar vertebra, and, furthermore, C7 has C6 characteristics and the spinous process characteristic of T2 is shifted to T3 or is present on both vertebrae. These effects presumably reflect the caudal shifts observed in the anterior expression boundaries of *Hox* genes in $Mll^{+/-}$ embryos. Interestingly, *Hoxa7* and *Hoxc9* transcripts cannot be detected in homozygous *Mll* null mutant embryos, despite the presence of structures normally exhibiting *Hox* expression, such as somites, spinal ganglia, limb buds, and the neural tube (69).

There are further apparent links between human embryo development and cancer, such as the rapidly expanding evidence for the involvement of *Hox* genes in the regulation of hematopoiesis and leukemia (4, 40, 58). Experimental dysregulation of *Hox* gene expression can lead to altered characteristics of blood cells or disturbance of blood cell development. For example, overexpression of *Hoxa7* and *Hoxa9* following retroviral gene transfer leads to myeloid leukemia in mice (49). Moreover, in cases of early childhood cancer, including AML and lymphoblastic leukemia, the incidence of a cervical rib (a posterior homeotic transformation of a cervical vertebra toward a thoracic-type vertebra) appears to be increased to about 25%, compared to approximately 2% in the general human population (57). This intriguing observation poses some important questions about the link between embryo-patterning processes and cancer and about the status of genes such as *AF9* in children with leukemia.

The molecular mechanism by which the MLL-AF9 fusion causes leukemia is obscure. The association of the C-terminal portion of the AF9 protein with N-terminal MLL sequences may target the fusion protein to sites not normally affected by AF9 through the DNA-binding properties of MLL, creating a novel *Hox* gene regulator. The induction of a chimeric MLL-AF9 protein in 32Dcl3 cells inhibits the up-regulation of *Hoxa7*, *Hoxb7*, and *Hoxc9* normally observed in the presence of granulocyte colony-stimulating factor when it substitutes for interleukin 3 (32). Similarly, MLL-ENL has been shown to transactivate the promoter of *Hoxa7*, an effect dependent on the DNA-binding properties of MLL and the C-terminal portion of ENL (56). Moreover, a recent study has revealed that the AF9 and ENL portions of MLL-AF9 and MLL-ENL, respectively, recruit HPC3, a member of the human Polycomb group of proteins (18), a group which regulates *Hox* gene expression and axial skeleton development. Further, the expression of an *Mll-AF9* fusion gene in mice disrupts myelopoiesis (15). These findings suggest that the two related fusion proteins, MLL-AF9 and MLL-ENL, may affect hematopoietic cell differentiation and proliferation through dysregulation of *Hox* genes, thereby leading to leukemogenesis.

ACKNOWLEDGMENTS

E.C.C. was a recipient of an LRF Gordon Pillar Studentship, and A.A. is the recipient of a Lady Tata Fellowship. This work was supported by the Medical Research Council.

We are indebted to Rob Krumlauf for invaluable help and advice with the in situ hybridization technique, for the *Hox* probes, and for his advice on embryo patterning. We also thank John O'Brien and Bill Wisden for interpretation of lacZ expression patterns. We thank Karen Douglas and Andrew Smith for pBS-TAG_3/IRESlacZ/lox/MC1neoPA/lox, Andrew McKenzie for PGKCre-pA, Vasanta Subramanian for the *Cdx-1* probe, and Alan Ashworth for *Cdx4* cDNA sequences.

REFERENCES

1. **Ayton, P. M., and M. L. Cleary.** 2001. Molecular mechanisms of leukemogenesis mediated by MLL fusion proteins. Oncogene Rev. **20:**5695–5707.
2. **Breen, T. R., and P. J. Harte.** 1993. Trithorax regulates multiple homeotic genes in the bithorax and Antennapedia complexes and exerts different tissue-specific, parasegment-specific and promoter-specific effects on each. Development **117:**119–134.
3. **Broeker, P. L., H. G. Super, M. J. Thirman, H. Pomykala, Y. Yonebayashi, S. Tanabe, N. Zeleznik-Le, and J. D. Rowley.** 1996. Distribution of 11q23 breakpoints within the MLL breakpoint cluster region in de novo acute leukemia and in treatment-related acute myeloid leukemia: correlation with scaffold attachment regions and topoisomerase II consensus binding sites. Blood **87:**1912–1922.
4. **Buske, C., and R. K. Humphries.** 2000. Homeobox genes in leukemogenesis. Int. J. Hematol. **71:**301–308.
5. **Cairns, B. R., N. L. Henry, and R. D. Kornberg.** 1996. TFG3/TAF30/ANC1, a component of the yeast SW1/SNF complex that is similar to the leukemogenic proteins ENL and AF-9. Mol. Cell. Biol. **16:**3308–3316.
6. **Cairns, B. R., Y. J. Kim, M. H. Sayre, B. C. Laurent, and R. D. Kornberg.** 1994. A multisubunit complex containing the SWI1/ADR6, SWI2/SNF2, SWI3, SNF5, and SNF6 gene products isolated from yeast. Proc. Natl. Acad. Sci. USA **91:**1950–1954.
7. **Carlson, M., and B. C. Laurent.** 1994. The SNF/SWI family of global transcriptional activators. Curr. Opin. Cell Biol. **6:**396–402.
8. **Cimino, C., M. C. Rapanotti, A. Biondi, L. Elia, F. Lo Coco, C. Price, V. Rossi, A. Rivolta, E. Canaani, C. M. Croce, F. Mandelli, and M. Greaves.** 1997. Infant acute leukemias show the same biased distribution of ALL1 gene breaks as topoisomerase II related secondary acute leukemias. Cancer Res. **57:**2879–2883.
9. **Cleary, M. L.** 1991. Oncogenic conversion of transcription factors by chromosomal translocations. Cell **66:**619–622.
10. **Collins, E. C., and T. H. Rabbitts.** 2002. The promiscuous *MLL* gene links chromosomal translocations to cellular differentiation and tumour tropism. Trends Mol. Med. 8:436–442.
11. **Condie, B. G., and M. R. Capecchi.** 1993. Mice homozygous for a targeted disruption of Hoxd-3 (Hox-4.1) exhibit anterior transformations of the first and second cervical vertebrae, the atlas and the axis. Development **119:**579–595.
12. **Corral, J., I. Lavenir, H. Impey, A. J. Warren, A. Forster, T. A. Larson, S. Bell, A. N. J. McKenzie, G. King, and T. H. Rabbitts.** 1996. An *Mll-Af9* fusion gene made by homologous recombination causes acute leukemia in chimeric mice: a method to create fusion oncogenes. Cell **85:**853–861.
13. **Cote, J., J. Quinn, J. L. Workman, and C. L. Peterson.** 1994. Stimulation of

GAL4 derivative binding to nucleosomal DNA by the yeast SWI/SNF complex. Science **265:**53–60.
14. **Djabali, M., L. Selleri, P. Parry, M. Bower, B. D. Young, and G. A. Evans.** 1992. A trithorax-like gene is interrupted by chromosome 11q23 translocations in acute leukaemias. Nat. Genet. **2:**113–118.
15. **Dobson, C. L., A. J. Warren, R. Pannell, A. Forster, I. Lavenir, J. Corral, A. J. H. Smith, and T. H. Rabbitts.** 1999. The *Mll-AF9* gene fusion in mice controls myeloproliferation and specifies acute myeloid leukaemogenesis. EMBO J. **18:**3564–3574.
16. **Domer, P. H., S. S. Fakharzadeh, C. S. Chen, J. Jockel, L. Johansen, G. A. Silverman, J. H. Kersey, and S. J. Korsmeyer.** 1993. Acute mixed-lineage t(4;11)(q21;q23) generates an MLL-AF4 fusion product. Proc. Natl. Acad. Sci. USA **90:**7884–7888.
17. **Fidanza, V., P. Melotti, T. Yano, T. Nakamura, A. Bradley, E. Canaani, B. Calabretta, and C. M. Croce.** 1996. Double knockout of the *ALL-1* gene blocks hematopoietic differentiation *in vitro*. Cancer Res. **56:**1179–1183.
18. **Garcia-Cuellar, M. P., O. Ziller, S. A. Schreiner, M. Birke, T. M. Winkler, and T. M. Slany.** 2001. The ENL moiety of the childhood leukemia-associated MLL-ENL oncoprotein recruits human Polycomb 3. Oncogene **20:**411–419.
19. **Gaunt, S. J., R. Krumlauf, and D. Duboule.** 1989. Mouse homeo-genes within a subfamily Hox-1.4, -2.6 and -5.1 display similar anteroposterior domains of expression in the embryo but show stage- and tissue-dependent differences in their regulation. Development **107:**131–141.
20. **Gu, Y., T. Nakamura, H. Alder, R. Prasad, O. Canaani, G. Cimino, C. M. Croce, and E. Canaani.** 1992. The t(4;11) chromosome translocation of human acute leukemias fuses the ALL-1 gene, related to Drosophila trithorax, to the AF-4 gene. Cell **71:**701–708.
21. **Hess, J. L., B. D. Yu, B. Li, R. Hanson, and S. J. Korsmeyer.** 1997. Defects in yolk sac hematopoiesis in *Mll*-null embryos. Blood **90:**1799–1806.
22. **Hoess, R. H., M. Ziese, and N. Sternberg.** 1982. P1 site-specific recombination: nucleotide sequence of the recombining sites. Proc. Natl. Acad. Sci. USA **79:**3398–3402.
23. **Hogan, B., R. Beddington, F. Costantini, and E. Lacy.** 1994. Manipulating the mouse embryo: a laboratory manual, 2nd ed. Cold Spring Harbor Laboratory Press, Cold Spring Harbor, N.Y.
24. **Horan, G. S., K. Wu, D. J. Wolgemuth, and R. R. Behringer.** 1994. Homeotic transformation of cervical vertebrae in Hoxa-4 mutant mice. Proc. Natl. Acad. Sci. USA **91:**12644–12648.
25. **Horan, G. S. B., E. N. Kovacs, R. R. Behringer, and M. S. Featherstone.** 1995. Mutations in paralogous *Hox* genes result in overlapping homeotic transformations of the axial skeleton: evidence for unique and redundant function. Dev. Biol. **169:**359–372.
26. **Horn, J. M., and A. Ashworth.** 1995. A member of the caudal family of homeobox genes maps to the X-inactivation centre region of the mouse and human X chromosomes. Hum. Mol. Genet. **4:**1041–1047.
27. **Hunt, P., M. Gulisano, M. Cook, M. H. Sham, A. Faiella, D. Wilkinson, E. Bonicelli, and R. Krumlauf.** 1991. A distinct Hox code for the branchial region of the vertebrate head. Nature **353:**861–864.
28. **Huret, J. L., P. Dessen, and A. Bernheim.** 2001. An atlas of chromosomes in hematological malignancies. Example: 11q23 and MLL. Leukaemia **15:**987–999.
29. **Iida, S., M. Seto, K. Yamamoto, H. Komatsu, A. Tojo, S. Asano, N. Kamada, Y. Ariyoshi, T. Takahashi, and R. Ueda.** 1993. MLLT3 gene on 9p22 in t(9;11) leukemia encodes a serine/proline rich protein homologous to MLLT1 on 19p13. Oncogene **8:**3085–3092.
30. **Isnard, P., N. Core, P. Naquet, and M. Djabali.** 2000. Altered lymphoid development in mice deficient for the mAF4 proto-oncogene. Blood **96:**705–710.
31. **Jeannotte, L., M. Lemieux, J. Charron, F. Poirier, and E. J. Robertson.** 1993. Specification of axial identity in the mouse: role of the Hoxa-5 (Hox1.3) gene. Genes Dev. **7:**2085–2096.
32. **Joh, T., Y. Hosokawa, R. Suzuki, T. Takahashi, and M. Seto.** 1999. Establishment of an inducible expression system of chimeric MLL-LTG9 protein and inhibition of Hox a7, Hox b7 and Hox c9 expression by MLL-LTG9 in 32Dcl3 cells. Oncogene **18:**1125–1130.
33. **Kaneko, Y., N. Maseki, N. Takasaki, M. Sakurai, Y. Hayashi, S. Nakazawa, T. Mori, M. Sakurai, T. Takeda, T. Shikano, and Y. Hiyoshi.** 1986. Clinical and hematologic characteristics in acute leukemia with 11q23 translocations. Blood **67:**484–491.
34. **Kessel, M.** 1992. Respecification of vertebral identities by retinoic acid. Development **115:**487–501.
35. **Kessel, M., R. Balling, and P. Gruss.** 1990. Variations of cervical vertebrae after expression of a Hox-1.1 transgene in mice. Cell **61:**301–308.
36. **Kessel, M., and P. Gruss.** 1991. Homeotic transformations of murine vertebrae and concomitant alteration of Hox codes induced by retinoic acid. Cell **67:**89–104.
37. **Kostic, D., and M. R. Capecchi.** 1994. Targeted disruptions of the murine Hoxa-4 and Hoxa-6 genes result in homeotic transformations of components of the vertebral column. Mech. Dev. **46:**231–247.
38. **Krumlauf, R.** 1994. *Hox* genes in vertebrate development. Cell **78:**191–201.
39. **Lavau, C., S. J. Szilvassy, R. Slany, and M. L. Cleary.** 1997. Immortalization and leukemic transformation of a myelomonocytic precursor by retrovirally transduced HRX-ENL. EMBO J. **16:**4226–4237.
40. **Lawrence, H. J., G. Sauvageau, R. K. Humphries, and C. Largman.** 1996. The role of HOX homeobox genes in normal and leukemic hematopoiesis. Stem Cells **14:**281–291.
41. **LeFranc, M.-P., A. Forster, R. Baer, M. A. Stinson, and T. H. Rabbitts.** 1986. Diversity and rearrangement of the human T cell rearranging γ genes: nine germ-line variable genes belonging to two subgroups. Cell **45:**237–246.
42. **Look, A. T.** 1997. Oncogenic transcription factors in the human acute leukemias. Science **278:**1059–1065.
43. **Mazo, A. M., D.-H. Huang, B. A. Mozer, and I. B. Dawid.** 1990. The trithorax gene, a trans-acting regulator of the bithorax complex in *Drosophila*, encodes a protein with zinc-finger domains. Proc. Natl. Acad. Sci. USA **87:**2112–2116.
44. **McGinnis, W., and R. Krumlauf.** 1992. Homeobox genes and axial patterning. Cell **68:**283–302.
45. **Meyer, B. I., and P. Gruss.** 1993. Mouse Cdx-1 expression during gastrulation. Development **117:**191–203.
46. **Morrison, A., L. Ariza-McNaughton, A. Gould, M. Featherstone, and R. Krumlauf.** 1997. *Hoxd4* and regulation of the group 4 paralogous genes. Development **124:**3135–3146.
47. **Morrissey, J., D. C. Tkachuk, A. Milatovitch, U. Francke, M. Link, and M. L. Cleary.** 1993. A serine/proline-rich protein is fused to HRX in t(4;11) acute leukemias. Blood **81:**1124–1131.
48. **Nakamura, T., H. Alder, Y. Gu, R. Prasad, O. Canaani, N. Kamada, R. P. Gale, B. Lange, W. M. Crist, P. C. Nowell, C. M. Croce, and E. Canaani.** 1993. Genes on chromosome 4, 9 and 19 involved in 11q23 abnormalities in acute leukemia share homology and/or common motifs. Proc. Natl. Acad. Sci. USA **90:**4631–4635.
49. **Nakamura, T., D. A. Largaespada, J. D. Shaughnessy, Jr., N. A. Jenkins, and N. G. Copeland.** 1996. Cooperative activation of Hoxa and Pbx1-related genes in murine myeloid leukaemias. Nat. Genet. **12:**149–153.
50. **Peterson, C. L., A. Dingwall, and M. P. Scott.** 1994. Five SWI/SNF gene products are components of a large multisubunit complex required for transcriptional enhancement. Proc. Natl. Acad. Sci. USA **91:**2905–2908.
51. **Pui, C. H., J. R. Kane, and W. M. Crist.** 1995. Biology and treatment of infant leukemias. Leukemia **9:**762–769.
52. **Rabbitts, T. H.** 1994. Chromosomal translocations in human cancer. Nature **372:**143–149.
53. **Rabbitts, T. H.** 1991. Translocations, master genes, and differences between the origins of acute and chronic leukemias. Cell **67:**641–644.
54. **Ramirez-Solis, R., H. Zheng, J. Whiting, R. Krumlauf, and A. Bradley.** 1993. Hoxb-4 (Hox-2.6) mutant mice show homeotic transformation of a cervical vertebra and defects in the closure of the sternal rudiments. Cell **73:**279–294.
55. **Rubnitz, J. E., J. Morrissey, P. A. Savage, and M. L. Cleary.** 1994. ENL, the gene fused with HRX in t(11;19) leukemias, encodes a nuclear protein with transcriptional activation potential in lymphoid and myeloid cells. Blood **84:**1747–1752.
56. **Schreiner, S. A., M. P. Garcia-Cuellar, G. H. Fey, and R. K. Slany.** 1999. The leukemogenic fusion of MLL with ENL creates a novel transcriptional transactivator. Leukemia **13:**1525–1533.
57. **Schumacher, R., A. Mai, and P. Gutjahr.** 1992. Association of rib anomalies and malignancy in childhood. Eur. J. Pediatr. **151:**432–434.
58. **Shen, W. F., K. Detmer, C. H. Mathews, F. M. Hack, D. A. Morgan, C. Largman, and H. J. Lawrence.** 1992. Modulation of homeobox gene expression alters the phenotype of human hematopoietic cell lines. EMBO J. **11:**983–989.
59. **Slany, R. K., C. Lavau, and M. L. Cleary.** 1998. The oncogenic capacity of HRX-ENL requires the transcriptional transactivation activity of ENL and the DNA binding motifs of HRX. Mol. Cell. Biol. **18:**122–129.
60. **Subramanian, V., B. I. Meyer, and P. Gruss.** 1995. Disruption of the murine homeobox gene Cdx1 affects axial skeletal identities by altering the mesodermal expression domains of Hox genes. Cell **83:**641–653.
61. **Super, H. J., N. R. McCabe, M. J. Thirman, R. A. Larson, M. M. Le Beau, J. Pedersen-Bjergaard, P. Philip, M. O. Diaz, and J. D. Rowley.** 1993. Rearrangements of the MLL gene in therapy-related acute myeloid leukemia in patients previously treated with agents targeting DNA-topoisomerase II. Blood **82:**3705–3711.
62. **Thomas, K. R., and M. R. Capecchi.** 1987. Site-directed mutagenesis by gene targeting in mouse embryo-derived stem cells. Cell **51:**503–512.
63. **Tkachuk, D. C., S. Kohler, and M. L. Cleary.** 1992. Involvement of a homolog of Drosophila Trithorax by 11q23 chromosomal translocations in acute leukemias. Cell **71:**691–700.
64. **Warren, A. J., W. H. Colledge, M. B. L. Carlton, M. J. Evans, A. J. H. Smith, and T. H. Rabbitts.** 1994. The oncogenic cysteine-rich LIM domain protein rbtn2 is essential for erythroid development. Cell **78:**45–58.
65. **Welch, M. D., and D. G. Drubin.** 1994. A nuclear protein with sequence similarity to proteins implicated in human acute leukemias is important for cellular morphogenesis and actin cytoskeletal function in *Saccharomyces cerevisiae*. Mol. Biol. Cell **5:**617–632.
66. **Wilkinson, D. G., and M. A. Nieto.** 1993. Detection of messenger RNA by *in situ* hybridisation to tissue sections and whole mounts. Methods Enzymol. **225:**361–373.

67. **Yagi, H., K. Deguchi, A. Aono, Y. Tani, T. Kishimoto, and T. Komori.** 1998. Growth disturbance in fetal liver hematopoiesis of Mll-mutant mice. Blood **92:**108–117.
68. **Yamamoto, K., M. Seto, Y. Akao, S. Iida, S. Nakazawa, M. Oshimura, T. Takahashi, and R. Ueda.** 1993. Gene rearrangement and truncated mRNA in cell lines with 11q23 translocation. Oncogene **8:**479–485.
69. **Yu, B. D., J. L. Hess, S. E. Horning, G. A. J. Brown, and S. J. Korsmeyer.** 1995. Altered *Hox* expression and segmental identity in *Mll*-mutant mice. Nature **378:**505–508.
70. **Ziemin-van der Poel, S., N. R. McCabe, H. J. Gill, R. Espinosa, Y. Patel, A. Harden, P. Rubinelli, S. D. Smith, M. M. LeBeau, J. D. Rowley, and M. O. Diaz.** 1991. Identification of a gene, *MLL*, that spans the breakpoint in 11q23 translocations associated with human leukemias. Proc. Natl. Acad. Sci. USA **88:**10735–10739.